



## Effect of Projection Height on Projection Collapse and Nugget Formation — A Finite Element Study

*An incrementally coupled analysis procedure can be used to develop improved procedures for determining weld conditions*

BY X. SUN

**ABSTRACT.** Projection welding is a variation of resistance welding in which current flow is concentrated at the point of contact with a local geometric extension of one (or both) of the parts being welded. These projections are used to concentrate heat generation at the point of contact, and, therefore, to generate a weld nugget faster and at a lower current level compared to conventional spot welding. Many factors affect the heat generation and projection collapse of the projection welding process. The effects of some of these factors, such as welding current, electrode force, and sheet material properties, have been studied using the coupled finite element simulation procedures in an earlier study by the author (Ref. 1). This paper is a sequel to the previous effort. It investigates the effect of projection height on projection collapse and nugget formation. Three projection designs with different projection heights were selected for 0.059-in., cold-rolled, low-carbon steel according to Ref. 2. The corresponding heat generation processes using one set of welding parameters were simulated using an incrementally coupled, thermal-electrical-mechanical modeling procedure (Refs. 1, 3). The predicted heating patterns were compared with the weld cross sections obtained from an earlier experimental approach using high-speed motion photography

(up to 6000 frames/s). The study offers fundamental understanding of the process physics for different projection designs and demonstrates again the effectiveness of an incrementally coupled modeling procedure.

### Introduction

Projection welding is an electrical resistance welding process in which resistance welds are produced at localized points in workpieces held under pressure between suitable electrodes. The projections are usually dome or cone shaped and are made with different designs according to recommendations of some standards. Although tests indicate satisfactory welds can be produced over a wide range of projection shapes, there is some ambiguity concerning optimum designs (Ref. 2). For example, a wide variety

of standards are recommended by different technical groups such as the American Welding Society and International Institute of Welding. In addition, different industries tend to establish their own projection design guidelines. It is intuitive that for different projection designs, the current paths will vary and this will, in turn, affect both projection collapse and the pattern of nugget formation. However, due to the complex flow paths for heat and electrical current and variations in material properties with temperature and phase changes, the projection welding process is difficult to analyze. When studying the effect of projection design on weld formation and weld quality, many earlier researchers had to rely on experimental techniques such as consecutive cross sectioning and high-speed motion photography (Refs. 2, 4).

With recent developments in finite element analysis and advances in computer technology, it is now possible to model the projection welding process and study current flow, heat generation, and projection collapse in quantitative detail. For example, the projection welding process was simulated with a coupled electrical-thermal-mechanical analysis procedure in Ref. 1, and the effects of different welding parameters, such as material grade, welding current, and electrode force, were investigated in great detail. In this study, the incrementally coupled analysis procedure developed in Refs. 1 and 3 was used to study

### KEY WORDS

Projection Welding  
Finite Element Analysis  
Projection Height  
Projection Design  
Welding Process  
Modeling  
Projection Collapse  
Nugget Growth

X. SUN is with Battelle Memorial Institute, Columbus, Ohio.

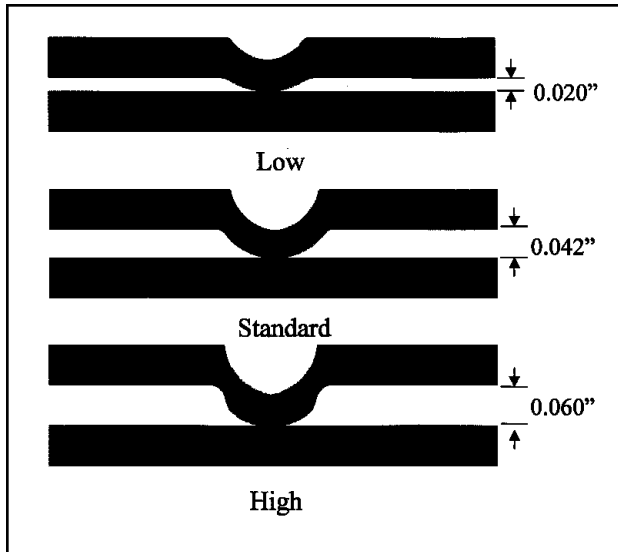


Fig. 1 — Cross sections of the three projection shapes studied.

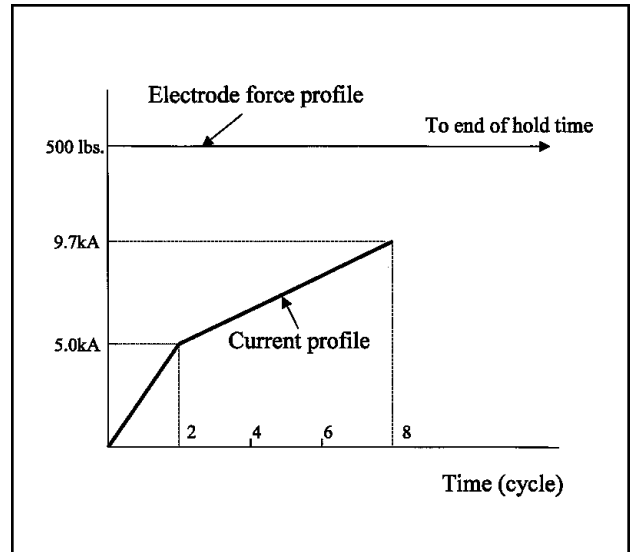


Fig. 2 — Illustration of welding parameters.

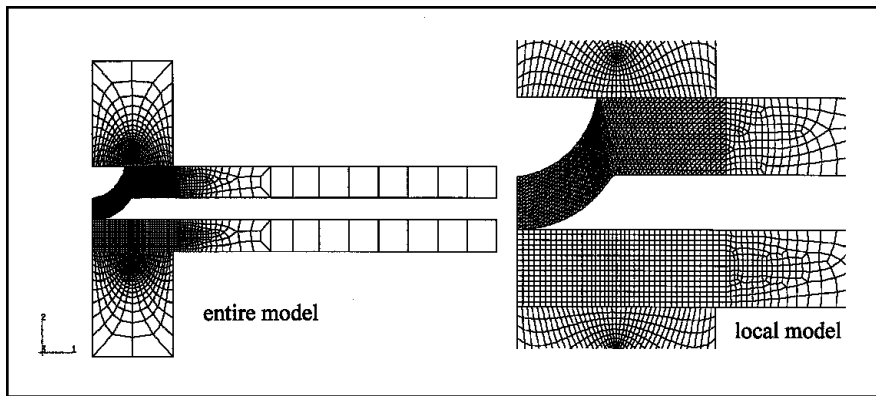


Fig. 3 — Typical finite element model for standard projection height.

the effect of projection height on heat generation and projection collapse for three different projection designs. A similar modeling procedure was also used to simulate the processes of resistance spot welding; it proved to be an effective tool in analyzing fundamental process physics.

To compare simulation with existing experimental results, the projection designs and sheet material studied in this work are the same as the ones examined in Ref. 2 using high-speed movies. Three projection heights were adopted for the H&R (Harris and Riley) projection in welding of 0.059-in., cold-rolled, low-carbon steel. This study's objective was to examine the current flow and heat generation process for the three projection heights in quantitative detail. This would, in turn, offer some insights on the optimization of projection heights and selec-

tion of different welding parameters. Comparison of predicted results with previous experimental measurements using high-speed motion photography (Ref. 2) also served as further validation of the modeling procedure.

### Projection Geometry and Model Description

Figure 1 shows cross sections of the three projection shapes for 0.059-in., SAE1010 cold-rolled steel as studied in Ref. 2. Projection heights vary from 0.02 to 0.06 in., and they are obtained by using H&R punch and die set T-4 (Refs. 2, 11). Notice the low projection is nearly uniform in thickness throughout, while higher projections showed increasingly thinner necked-down regions.

The sheet material SAE 1010 had a room temperature nominal yield strength

of 270 MPa, ultimate strength of 310 MPa, and elongation of 32% (Refs. 10, 14). Its physical (electrical and thermal) and mechanical properties in elevated temperatures were found in Refs. 5–7. A true stress and strain curve was used with no strain rate sensitivity (Ref. 1). It should also be mentioned the analysis did not take into consideration the residual stress states in the projection area due to the punching process, nor did it consider the effect of work hardening on the material around the projection area.

The electrodes used were flat-faced RWMA Class III electrodes with a face radius of 0.16 in. (4 mm). The same welding parameters were used for the three projection designs: welding current of 9.7 kA with bilinear up-slope control and constant electrode force of 500 lb — Fig. 2. The current is an approximation of the current profile documented in Fig. 2 of Ref. 2. By specifying the constant electrode force, perfect machine follow-up was assumed. Only 8 cycles of weld time were used, as opposed to 30 cycles used in Ref. 2. This was because projection collapse occurred only during the early stage of the welding process. For all three cases, projection collapse was completed by the eighth cycle and nugget growth beyond that point was similar to that of the resistance spot welding process.

The theoretical framework and associated finite element modeling procedure using commercial code [*e.g.*, ABAQUS (Ref. 13)] for the projection welding process are presented in Refs. 1 and 3. A typical finite element mesh is shown in Fig. 3 for the standard projection with three-node linear elements in the projection area and four-node linear



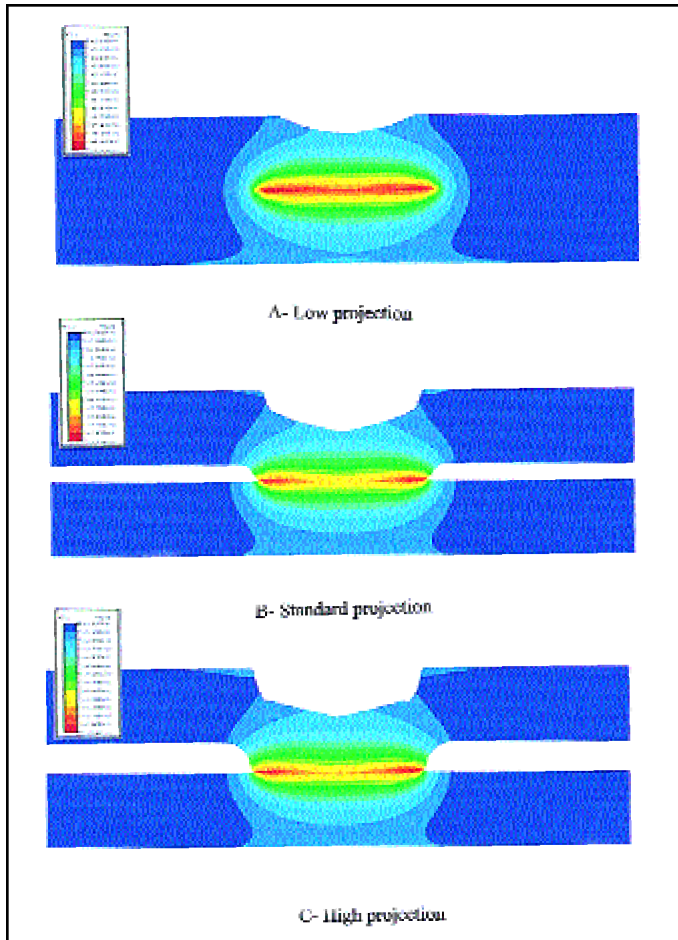


Fig. 7 — Temperature distribution at the end of the second welding cycle.

a certain time increment was then imposed as thermal loading conditions for the subsequent thermal-mechanical analysis module. This updating procedure repeated itself for every  $\frac{1}{6}$  cycle (Ref. 1), until the entire welding cycle was totally completed.

## Analysis Results

### Squeeze Cycle

At the end of the squeeze cycle, cold collapse of the projection occurred and an area of intimate mechanical contact on the faying interface was established for the subsequent electrical current to pass through. The amount of cold collapse depends on the electrode force and the individual projection design. For example, Fig. 4 shows the contour plots of the stress component on the deformed shapes for the three projection heights after squeeze cycle. As illustrated in Fig. 4, the faying interface contact radius established due to the squeezing force decreases with increasing projection heights. For the lowest projection height,

the projection collapsed almost entirely and the contact pressure at the upper electrode-projection interface observed the highest value among the three cases considered.

### Initial Welding Cycles and Projection Collapse

Because of the differences in the established faying interface contact area for the three projection heights, the corresponding current density distributions, and therefore the rate of heat generation, were also different for the three cases considered in the initial welding cycles. The evolution of the faying interface contact radius during the first two cycles is compared in Fig. 5 for the three cases considered. For all three projection shapes, the contact radius on the faying interface increased monotonically with time during the first two cycles. This was another manifestation of the gradual projection collapse process. The lowest pro-

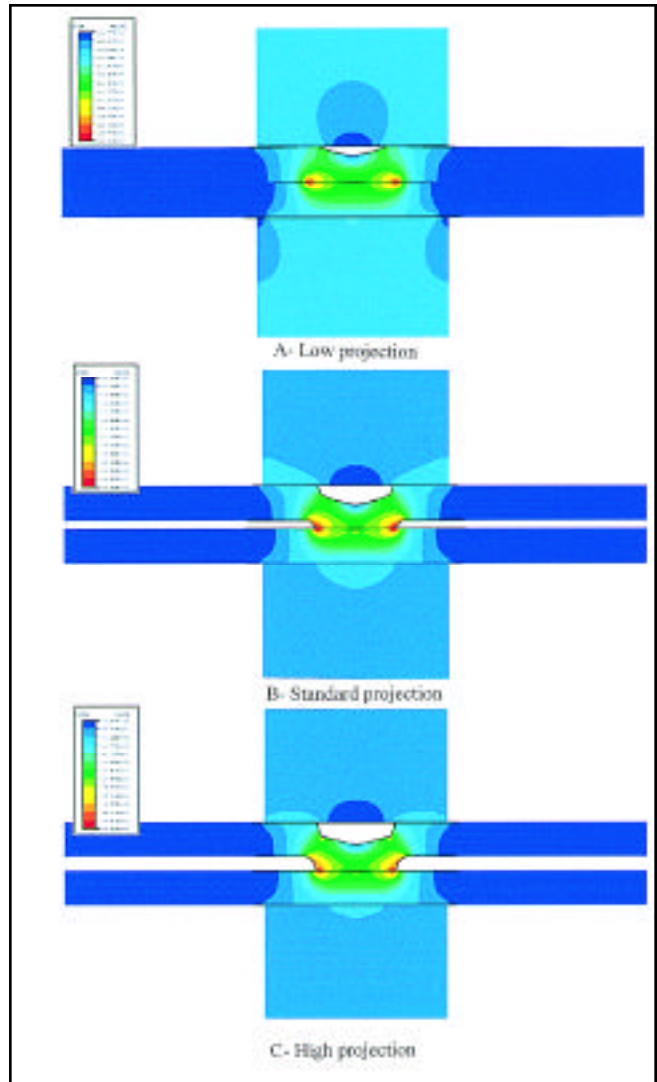


Fig. 8 — Current density distribution at the end of the second welding cycle.

jection consistently had the highest contact radius among the three cases. The contact radius of the standard projection was higher than the highest projection during the squeeze cycle and subsequent first cycle of welding. After the first cycle, the contact radius for the highest projection caught up with the standard projection because of local heating-induced material softening along the periphery of the faying interface.

The change of contact radius during the first two cycles for the lower electrode-sheet interface is shown in Fig. 6 for the three cases considered. The trend was fundamentally different from that of spot welding using flat-faced electrodes (Ref. 8). Before the end of the first welding cycle, the electrode-sheet interface radius increased with time due to the projection collapse process and the corresponding increase of the faying interface contact area.



nugget penetration on the upper sheet was predicted for the lowest projection because of the lower magnitude of current density on the faying interface.

It is interesting to note that, with increasing projection heights, the effects of projection collaring and projection digging (into the lower workpiece) were more prominent. That is, when a high projection was used, some of the material composing the projection at the periphery of the faying interface was squeezed out around the edge of the weld, forming an extruded collar — Figs. 7 and 8. This observation was again consistent with many previous experimental findings (Ref. 10).

## Discussion and Conclusions

In this paper, the incrementally coupled finite element analysis procedure is used as a modeling tool to study the effect of projection design on the projection collapse process and heat generation patterns during the early stage of the projection welding process. Three projection designs from an earlier experimental study were adopted, and the predicted results on nugget formation and projection collapse compared reasonably well with the available experimental data obtained through high-speed movies.

This demonstrates again that the incrementally coupled analysis procedure developed in Refs. 1 and 3 can be used as a powerful tool to study the detailed process physics of a highly dynamic, coupled process such as projection welding, and provides some quantitative understanding and guidelines about projection design and welding parameter selection. With this tool, it is possible to develop improved procedures for determining weld conditions, requiring only a nominal amount of experimental work as a means of verification.

It was found that interfacial contact behavior (contact area change due to projection collapse) played a critical role in the initial heating process in projection welding. If an extremely high projection is used, the rate of localized heating is faster than the rate of projection collapse on the periphery of the faying interface and as a result, weld collaring and expulsion will occur during the early welding cycles. On the other hand, if a low projection height is used, premature collapse of the projection will cause the contact area to be large and, therefore, reduce the current density on the faying interface and delay nugget formation. The dynamic balance between projection collapse and heat generation must

therefore be maintained to optimize the projection welding process. To this end, the analysis procedure can be used as a predictive tool to optimize the projection design for a specific sheet material to ensure nugget size and weld quality. Another application area of this tool is in the selection of different welding parameters, such as welding current, electrode force, and sheet material properties. These effects have been discussed in Ref. 1, and will not be repeated here.

It should be mentioned that no material strain rate sensitivity was included in the current simulation results. This was due to the lack of rate data for the elevated temperature under the deformation rate considered. Should such data become available, it can be easily incorporated in the modeling procedure. No work-hardening effect of the projection material due to the punching process was taken into consideration and the entire projection was considered to be stress and strain free prior to the welding process. Also, perfect electrode follow-up was assumed for the welding machine, and the magnetic stirring effect, as observed in many earlier high-speed movie studies, was not considered (Ref. 4).

## References

1. Sun, X. 2000. Modeling of projection welding processes using coupled finite element analyses. *Welding Journal* 79(9): 244-s to 251-s.
2. Cunningham, A., and Begeman, M. L. 1966. Effect of projection height upon weld quality and strength. *Welding Journal* 45(1): 26-s to 30-s.
3. Sun, X., and Dong, P. 2000. Analysis of aluminum resistance spot welding processes using coupled finite element procedures. *Welding Journal* 79(8): 215-s to 221-s.
4. Cunningham, A., and Begeman, M. L. 1965. A fundamental study of projection welding using high speed photography. *Welding Journal* 44(8): 381-s to 384-s.
5. *Metals' Handbook*, 9th ed., Vols. 1 and 2. 1978. Properties and selections: Irons and steels.
6. *High-Temperature Property Data: Ferrous Alloys*. 1988. Metals Park, Ohio: ASM International.
7. *Physical Constants of Some Commercial Steels at Elevated Temperatures*. 1953. Edited by The British Iron and Steel Research Association. London U.K.: Butterworths Scientific Publications.
8. Li, M. V., Dong, P., and Kimchi, M. 1997. Modeling of contact resistance during resistance spot welding. *Proc. 7th Int. Conf. on Computer Tech. in Welding*. Ed. T. Stewert. NIST Special Publication 923, U.S. Department of Commerce, pp. 423-435.
9. Hess, W. F., Childs, W. J., and Underhill,

R. F., Jr. 1949. Further studies in projection welding. *Welding Journal* 28(1): 15-s to 23-s.

10. Hess, W. F., and Childs, W. J. 1947. A study of projection welding. *Welding Journal* 27(12): 712-s to 723-s.

11. Harris, J. F., and Riley, J. J. 1961. Projection welding low-carbon steel using embossed projects. *Welding Journal* 40(4): 363-s-376-s.

12. Adams, J. V., Matthews, G. N., and Begeman, M. L. 1965. Effect of projection geometry upon weld quality and strength. *Welding Journal* 44(10): 466-s to 470-s.

13. *ABAQUS/Standard and ABAQUS/Explicit User's Manuals*, Version 5.8. Hibbitt, Karlsson & Sorensen, Inc.

14. Nippes, E. F., and Gerken, J. M. 1952. Projection welding of steel in heavy gages and in dissimilar thicknesses. *Welding Journal* 31(3): 113-s to 125-s.

## REPRINTS REPRINTS

To Order Custom Reprints  
of Articles in the

*Welding Journal*

Call Denis Mulligan  
at (800) 259-0470

## REPRINTS REPRINTS